Results in Geochemistry 7-8 (2022) 100017

Contents lists available at ScienceDirect

Results in Geochemistry

journal homepage: www.journals.elsevier.com/results-in-geochemistry

Southeast Asian dust flux reconstructed using accurately dated stalagmite thorium concentrations

T. Verniers [a], H. Couper [b], F.A. Lechleitner [c], J.U.L. Baldini [a,*]

[a] Department of Earth Sciences, Durham University, Durham DH1 3LE, UK
[b] Department of Earth Sciences, University of Oxford, Oxford OX1 3AN, UK
[c] Department of Chemistry, Biochemistry and Pharmaceutical Sciences and Oeschger Centre for Climate Change Research, University of Bern, Freiestrasse 3, Bern 3012, Switzerland

ARTICLE INFO

Keywords:
Stalagmite
Speleothem
Dust
Wind deposits
Climate
Paleoclimate
Thorium

ABSTRACT

Mineral dust flux is an important component of the global climate system, but chronological uncertainties complicate interpretations of the timing and magnitude of paleo-dust fluxes. This study establishes a correlation between modern satellite-derived atmospheric dust concentration data and stalagmite thorium concentrations (from published records of stalagmites growing over the last 500 years), and subsequently applies this relationship to reconstruct Asian dust flux during the late Pleistocene using published records. Thorium is an element often associated with mineral dust, and because most stalagmite records are dated using uranium-thorium disequilibrium techniques, a spatiotemporally large, yet untapped, database of thorium concentrations exists. Specifically, 194 thorium records from South-East (SE) Asian stalagmites were compiled to produce a composite SE Asian dust flux record for the past 100,000 years. The new dust flux record is consistent with the perspective that dust flux is a function of westerly wind strength across Asia and regional aridity. Dansgaard-Oeschger (D-O) event expression within the median stalagmite ^{232}Th record is variable, with several D-O events evident within stalagmite δ^{18}O records not evident within the new dust record. This may reflect East Asian Summer Monsoon (EASM) moisture source region Sea Surface Temperature (SST) variability (affecting stalagmite δ^{18}O) but stable westerly wind regime (resulting in invariant ^{232}Th concentrations) or the fact that these events were too brief to trigger biome shifts. This study presents encouraging first results suggesting that stalagmite thorium concentrations partially reflect dust flux over cave sites. Although here we use a compilation of records, and the spread of data within each time slice is high, future studies at well-understood cave sites where thorium input to the cave is predominantly via dry deposition may require only single stalagmites to produce adequate absolutely dated dust reconstructions.

1. Introduction

Wind-blown mineral dust is highly influential for the Earth's climate, affecting solar radiation reaching the Earth's surface and acting as a significant source of nutrients for remote oceanic locations (Martinez-Garcia et al., 2014). Dust emission, distribution, and deposition comprises a feedback loop involving the hydrological cycle, vegetation growth, surface winds, and changing climatic conditions (Choobari et al., 2014). Understanding the connections between atmospheric dust and climate therefore improves simulations and constructions of global Earth System Models (Albani et al., 2018). 81% of current global dust emissions are produced by natural sources (Chen et al., 2018) and reconstructing spatiotemporal distributions of ancient dust fluxes enhances our understanding of the mechanisms controlling dust fluxes, as well as how dust fluxes contribute to climate shifts (e.g., via iron fertilization, etc.). Dust aerosols interact both directly and indirectly with the Earth's radiation budget by affecting the atmosphere's radiative flux at both solar and thermal wavelengths (Miller et al., 2014). Dust aerosols in the lower levels of the atmosphere can indirectly influence the earth's energy budget by affecting cloud and particle size (Allen, 2017). Through analysis of lidar and radiosonde observations, Mikami et al. (2006) also found that dust particles act as nucleation sites for ice particles at the ice-saturated region of the atmosphere. By acting as cloud condensation and ice nuclei, dust aerosols affect cloud lifetime

* Corresponding author.
E-mail address: james.baldini@durham.ac.uk (J.U.L. Baldini).

https://doi.org/10.1016/j.ringeo.2022.100017
Received 22 January 2022; Received in revised form 29 July 2022; Accepted 1 August 2022
Available online 2 August 2022

and albedo, impacting how clouds reflect and absorb terrestrial radiation (Allen, 2017). Mineral dust deposition can also greatly reduce surface albedo (e.g., Albani et al. 2018).

Despite its importance, the reconstruction of the paleo-dust flux is hampered by archives that are either not widely distributed geographically and/or are not easily dateable. Pure mineral dust is almost insoluble and is quantifiable in sedimentary deposits (such as loess) as the insoluble dust number and volume concentration (Guo et al., 2009). These measurements allow dust mass accumulation rates (DMAR) derivation when combined with chronological information from radiocarbon or luminescence ages in loess deposits (Ujvari et al., 2010). However, these methods are subject to large uncertainties and are limited in their temporal range (Liu et al., 1985) because soil horizon age uncertainties translate to their respective DMAR calculation. As a result, dust flux reconstructions from loess are limited in their temporal coverage and are associated with high levels of chronological uncertainty.

Stalagmites are a potentially suitable archive for dust flux reconstructions because they are globally ubiquitous and amenable to high precision radiometric dating using uranium-thorium methods. Unlike uranium (U), thorium (Th) is insoluble and is not transported or deposited authigenically by groundwater as the speleothem forms. Ideally (for U-Th dating), no Th is initially present in newly deposited stalagmite carbonate, with ^{230}Th accumulation only occurring following the radiogenic decay of U. ^{232}Th is not part of the ^{238}U decay chain, and any ^{232}Th within a stalagmite reflects detrital material either flushed into the cave via dripwater (Wong & Breecker, 2015) or advected into the cave via air circulation (Jamieson et al., 2015; Baldini et al., 2012). ^{232}Th concentrations are routinely measured during uranium-series dating analyses to assess the accuracy of the date and to quantify allogenic initial ^{230}Th concentrations for any correction (Hellstrom, 2003). Consequently, every U-Th date has an associated ^{232}Th concentration value; this study utilizes a compilation of published stalagmite ^{232}Th concentration data to reconstruct ancient dust fluxes.

2. Methodology

We compile the corrected U-Th ages and associated ^{232}Th concentrations of 435 globally distributed stalagmites synthesized in the Speleothem Isotopes Synthesis and Analysis database version 1 (SISALv1; Atsawawaranunt et al., 2018) (Fig. 1). Areas of high record density include SE Asia and Europe, whereas Northern Africa, central Australia, and higher latitudes have noticeably limited coverage. A fundamental requirement for stalagmite growth is sufficient meteoric precipitation to allow for effective infiltration into the subsurface (Vaks et al., 2010), explaining the lack of stalagmite occurrence in hyper-arid regions, such as the Sahara Desert and central Australia. Equally, stalagmite growth is strongly correlated to temperature and the amount of CO_2 available in the soil (Baldini et al., 2005), explaining the lack of samples at high latitudes, along with factors such as ice sheet cover restricting growth.

2.1. Stalagmite thorium and Dust Column Mass Density (DCMD) correlation

Here, we demonstrate the presence of a relationship between Dust Column Mass Density (DCMD), a measure of mineral dust in the atmosphere, and mean stalagmite ^{232}Th concentrations over the recent past. DCMD data were obtained from the *Modern-Era Retrospective analysis for Research and Applications version 2* (MERRA-2) dataset, a NASA atmospheric reanalysis for the satellite era using the Goddard Earth Observing System Model, Version 5 (GEOS-5) with its Atmospheric Data Assimilation System (ADAS), version 5.12 (GMAO, 2015). The data were extracted as area-averaged time-series of a monthly temporal resolution, for an area of 1° squared containing each cave site. A mean DCMD value for the last 20 years was calculated per grid square and used to evaluate correlations with recent ^{232}Th concentrations for that cave site.

For inclusion within the calibration dataset, a stalagmite required a minimum of two U-Th dates within the last 500 years, allowing for the calculation of a mean ^{232}Th concentration. Additionally, detrital features (clear flooding horizons, macro-scale detrital layers, etc.) were assessed on images of the stalagmites, and any stalagmites with visible detrital components (n = 31, Table S4) were omitted from the analysis. Ultimately, 56 samples met these criteria. Ideally, the satellite and U-Th calibration data would derive from a common interval, but the satellite dataset's brevity precludes the extraction of a meaningful ^{232}Th concentration dataset (because the data resolution is typically centennial-scale). The threshold of a minimum of two dates over the past 500 years was chosen to maximise the calibration dataset's population while also attempting to avoid major climate transitions. To minimize the influence of isolated events (e.g., flooding, hydrological pulses, etc.),

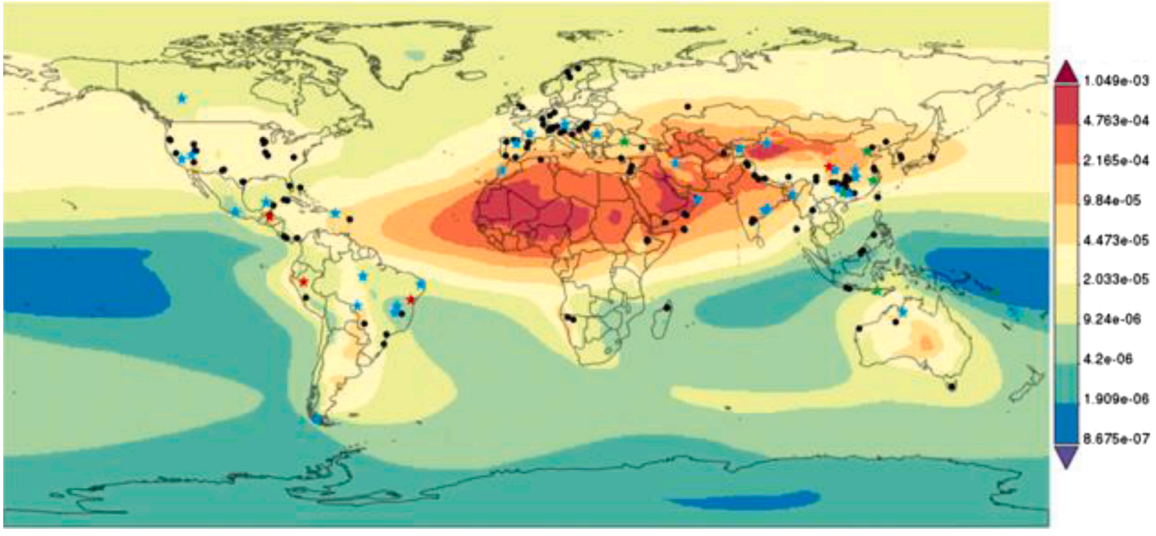

Fig. 1. The distribution of stalagmites used in this study. Sites marked with a star symbol are used in the calibration curve. Blue stars indicate single stalagmites, red stars indicate multiple asynchronous samples from the same cave site, and green stars highlight caves where multiple stalagmites were combined to form a cave data point (see Supplemental Information). Stalagmites marked by black circles are not used in the calibration curve but are available for dust reconstructions. The base map shading illustrates mean Dust Column Mass Density (kg m^{-2}) between January 2000 and 2020. Data is sourced from the public EarthData Giovanni NASA database.

^{232}Th concentrations higher than one standard deviation from the mean of the stalagmite were excluded from the calibration dataset. Where multiple stalagmites within the same cave met the criteria for inclusion in the calibration dataset, a single mean value was calculated for the cave by compiling the two stalagmite data sets (Supplemental Table S1). The same procedure as applied to single stalagmites was followed when calculating compiled mean ^{232}Th concentrations from a region with a single DCMD value.

2.2. Stalagmite ^{232}Th concentrations as a proxy for Asian dust flux

SE Asia was chosen because of the large number of well-dated stalagmite records produced from that region and the existence of other regional dust flux records (e.g., from loess) which facilitate comparison. To produce a continuous reconstruction of Asian dust flux, the ^{232}Th concentrations of 194 stalagmites from SE Asia (see Supplemental Information, Table S3) were linearly interpolated at a decadal resolution and compiled into a single curve. Gaps of more than 5000 years in a stalagmite record were not interpolated across because these were deemed too large to accurately interpolate. A median value for all stalagmites available was calculated for each 10-year time slice. We used the median instead of the mean to minimise the impact of data points with anomalously high ^{232}Th concentrations that potentially reflect anomalous events rather than regional climate trends.

3. Results and discussion

3.1. Global calibration curve

The final calibration dataset included 56 stalagmites from 48 caves (Fig. 1); once stalagmites from the same cave and/or DCMD grid square are combined this yields 41 thorium concentration datapoints for the calibration curve. The relationship between mean ^{232}Th concentrations from this dataset and mean DCMD values at the cave sites is strong and highly significant ($r^2 = 0.38$, $p < 0.0001$, $n = 41$) (Fig. 2).

The global calibration curve strongly suggests that speleothem ^{232}Th concentrations are partially linked to DCMD values, and that atmospheric dust is either i) blown directly into the cave by dynamic ventilation processes (Dredge et al., 2013; Jamieson et al., 2015) or ii) flushed into the cave by percolation water (Baldini et al., 2012). We find no correlation between stalagmite ^{232}Th concentrations and Total Surface Precipitation (TSP) values from the MERRA-2 dataset using a 1° grid centered around each cave site, from monthly values recorded since January 1, 2000 ($r^2 = 0.04$, $p = 0.78$, $n = 41$).

3.2. Mechanism for dust flux recording in caves

The low correlation between rainfall and median stalagmite ^{232}Th record across the calibration dataset strongly suggests that increased mechanical transport of soil colloidal material via percolating drip water is not the dominant control on stalagmite ^{232}Th concentrations. Instead, we suggest that stalagmite ^{232}Th predominantly reflects aeolian dust transport and regional ambient dustiness. Nearly all caves ventilate either on seasonal or daily timescales (Baldini et al., 2006; James et al., 2015), and it is likely that dust entering the cave via ventilation (Dredge et al., 2013) is deposited not only on the growing stalagmite, but also on the walls and ceiling of the cave (Jamieson et al., 2015). Percolation (and potentially condensation) of water then transports dust particles to the growing stalagmite where they are incorporated into the deposited calcite. Cave-specific ventilation dynamics, drip hydrology, sampling bias (both in stalagmite selection and in the selection of dating locations within a sample), proximity to cave streams, and other factors will however likely impact ^{232}Th concentrations and contribute to variability in the signal and noise within the calibration dataset. A consequence of these observations is that if stalagmite ^{232}Th values are not related to transport of local sediment particles via percolating water, the use of local sediment geochemical composition when determining the detrital fraction for U-Th dating requires re-evaluation. Temporal variability in dust composition affecting the cave site is potentially more important than previously thought and may require consideration in U-Th dating correction.

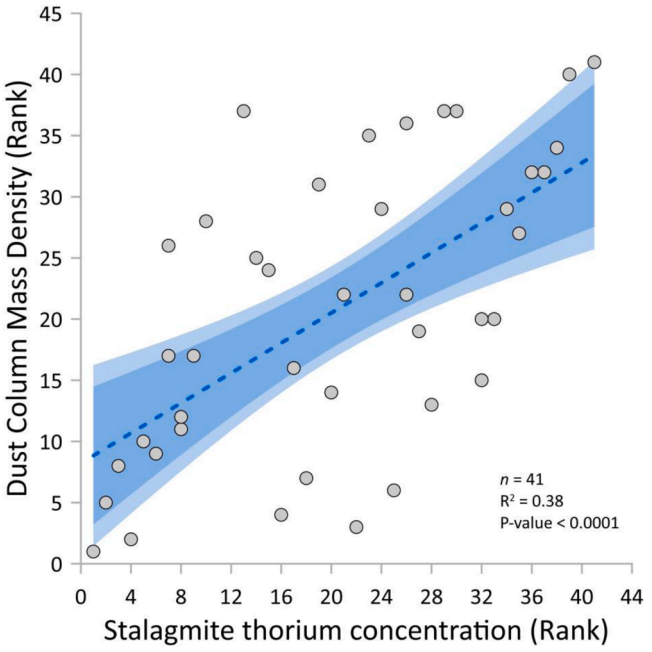

Fig. 2. A Spearman's Rank Correlation plot of modern Dust Column Mass Density (DCMD) (mean value of the previous 20 years) from the EarthData Giovanni NASA database and recent (mean over the last 500 years) stalagmite thorium concentrations (Table S1). The blue envelopes represent the 95% (dark blue) and 99% (light blue) confidence intervals, showing the estimated ranges of regression lines representing other samples drawn from the same statistical population (based on 5000 iterations for each interval). The envelopes demonstrate that there is a very high likelihood that the relationship between stalagmite thorium concentrations and DCMD is positive.

The good correlation between dust and DCMD values globally suggests that ^{232}Th records from other archives should be investigated for their potential to reconstruct dust flux, particularly in areas with few stalagmites. Ice cores dated by ^{234}U recoil ages (Aciego et al., 2011) could, if combined with ^{232}Th measurements, provide a complementary high latitude equivalent to the stalagmite dust archive.

3.3. Asian dust flux reconstruction and comparison with existing records

Our calculation of median speleothem ^{232}Th from the SE Asia region shows substantial ^{232}Th concentrations variability over the past 600 ka (Fig. 3), but the number of available records decreases substantially after ca. 25 ka BP and then remains about constant until ca. 120 ka BP. Here we focus our analysis on the most robust portion of the record, the late Pleistocene period (0–120 ka BP), but the potential exists to use this new technique to produce a record extending back to ~600 ka.

Despite the low number of data points over the older portions, over the last 500 ka the median stalagmite ^{232}Th record suggests that SE Asia was dustier during glacials than interglacials (Fig. 3), consistent with previous studies (Yancheva et al., 2007). Over the well-resolved last 20 ka BP, the median stalagmite ^{232}Th record displays similarities with the winter monsoon record from Lake Huguang Maar, China (Fig. 4) (Yancheva et al., 2007). Because northerly winter monsoon winds are the main input of aeolian input to the Lake Huguang Maar, this record reflects ambient dustiness over time. The similarities between our median stalagmite ^{232}Th record and the Huguang Maar record reinforce our interpretation that median stalagmite ^{232}Th values are an effective

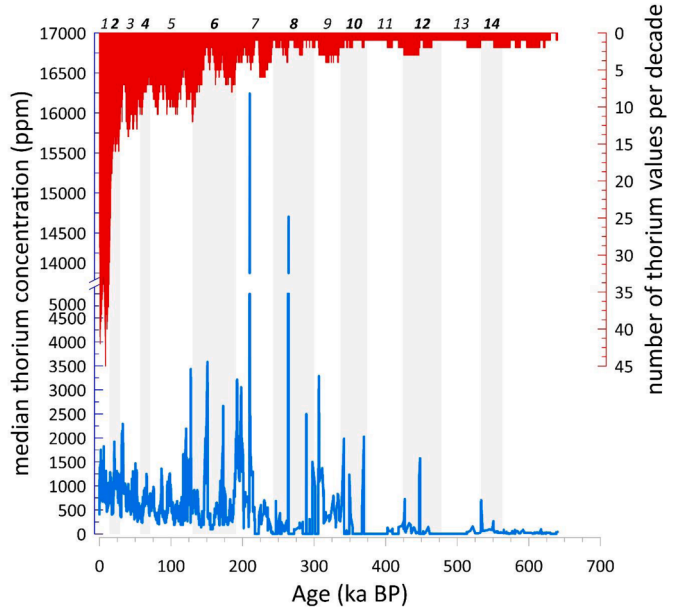

Fig. 3. The median thorium concentration record compiled from 194 Asian stalagmite thorium datasets (bottom panel) and a histogram illustrating the number of values compiled per decade (top panel). Note the break in the y-axis in the bottom panel. Please see SI (Table S2) for sources and references. Alternating grey and white boxes represent Marine Isotope Stages (MIS) for reference (Lisiecki & Raymo, 2005), with MIS number shown along top.

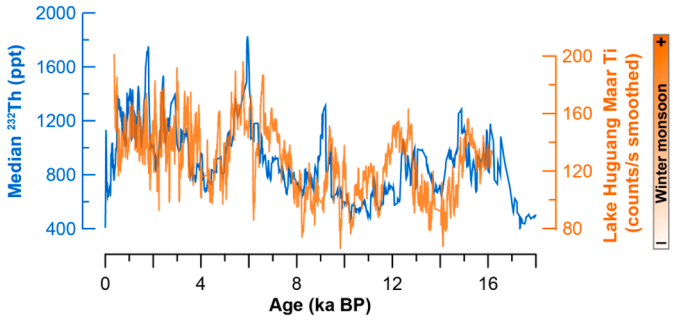

Fig. 4. Comparison between median ^{232}Th East Asia dust flux reconstruction from stalagmites (blue line) over the interval 0–18 ka BP with the Lake Huguang Maar Ti record (smoothed using a 9-point triangular window; (Yancheva et al., 2007), orange line). The Lake Huguang Maar record is interpreted as reflecting the strength of the winter monsoon, when aeolian input from the Chinese Loess Plateau to the lake is dominant.

tracer for windblown dust.

On centennial-millennial timescales, we find a clear relationship between the Asian dust flux reconstruction, global ice volume (reflected in sea level records), Chinese stalagmite $\delta^{18}O$, and the Greenland NGRIP ice core $\delta^{18}O$ record (Figs. 5 and 6). For example, lower sea level reflects high ice volume and colder conditions in Greenland (lower ice core $\delta^{18}O$) and across the Northern Hemisphere, resulting in a weakened EASM (elevated SE Asian stalagmite $\delta^{18}O$), and enhanced westerly wind strength over SE Asia (elevated median ^{232}Th) (Fig. 5). Therefore, the link between ice volume and our median ^{232}Th record likely reflects ice volume's influence on westerly wind position and SE Asia winter monsoon strength, which also affects dust flux to SE Asia. By looking at the correlation between EASM $\delta^{18}O$ and our median ^{232}Th record compared with sea level, it is possible to further evaluate the control of ice volume on the dust/$\delta^{18}O$ relationship (Fig. 7). Although no strong relationship exists ($R^2 = 0.21$, $p = 0.01$, $n = 28$), in general during high ice volume intervals the correlation between dust and stalagmite $\delta^{18}O$ is

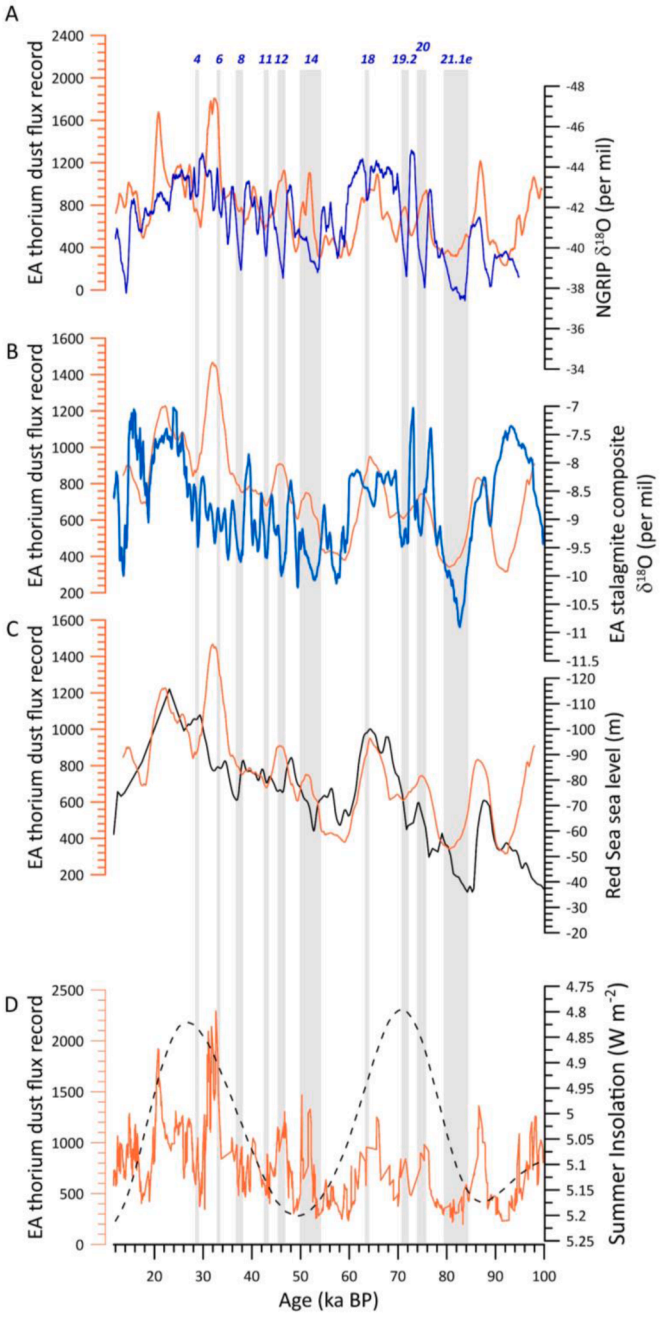

Fig. 5. The median ^{232}Th East Asia dust flux reconstruction (orange in all panels) over the interval 10-100 ka BP compared with other datasets: (A) NGRIP $\delta^{18}O$ (purple, 41-pt MA) (North Greenland Ice Core Project, NGICP Members, 2004) and median ^{232}Th East Asia dust flux reconstruction (orange, 99-pt MA), (B) a compiled EA stalagmite $\delta^{18}O$ record (blue, 13-pt MA) (Cheng et al., 2016) and median ^{232}Th East Asia dust flux reconstruction (orange, 401-pt MA), (C) Red Sea sea level reconstruction (black) (Siddall et al., 2003) and median ^{232}Th East Asia dust flux reconstruction (orange, 401-pt MA) and (D) NH summer insolation (65°N) reconstruction (dashed grey line) (Huybers, 2006) and median ^{232}Th East Asia dust flux reconstruction (orange, no MA used). Major D-O events are highlighted with grey shading.

most negative, suggesting that Dansgaard-Oeschger (D-O) events (abrupt millennial-scale warming events) occurring during high ice volume conditions are characterised by a weaker EASM and weaker westerly wind strength over SE Asia (lower median ^{232}Th) (Fig. 7). On the other hand, intervals characterised by lower ice volume (i.e., higher global temperatures) experienced stronger EASM rainfall and weaker

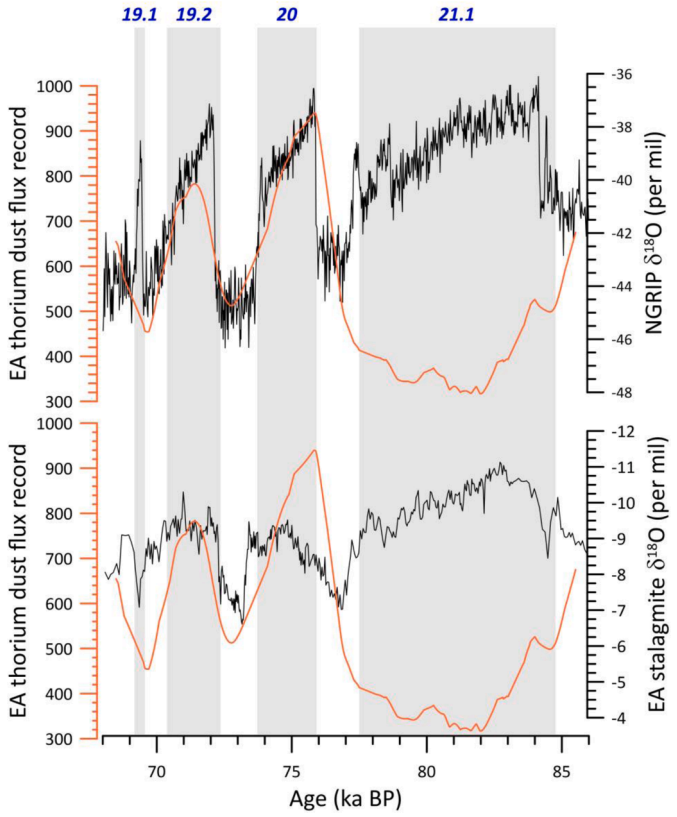

Fig. 6. The median ^{232}Th East Asia dust flux reconstruction (orange, 99-point moving average) over the interval 68–76 ka BP compared with: (*Top panel*) NGRIP δ^{18}O (purple, 41-pt MA) (North Greenland Ice Core Project, NGICP Members, 2004), (*Bottom panel*) a compiled EA stalagmite δ^{18}O record (blue, 13-pt MA) (Cheng et al., 2016). D-O events are highlighted with grey shading.

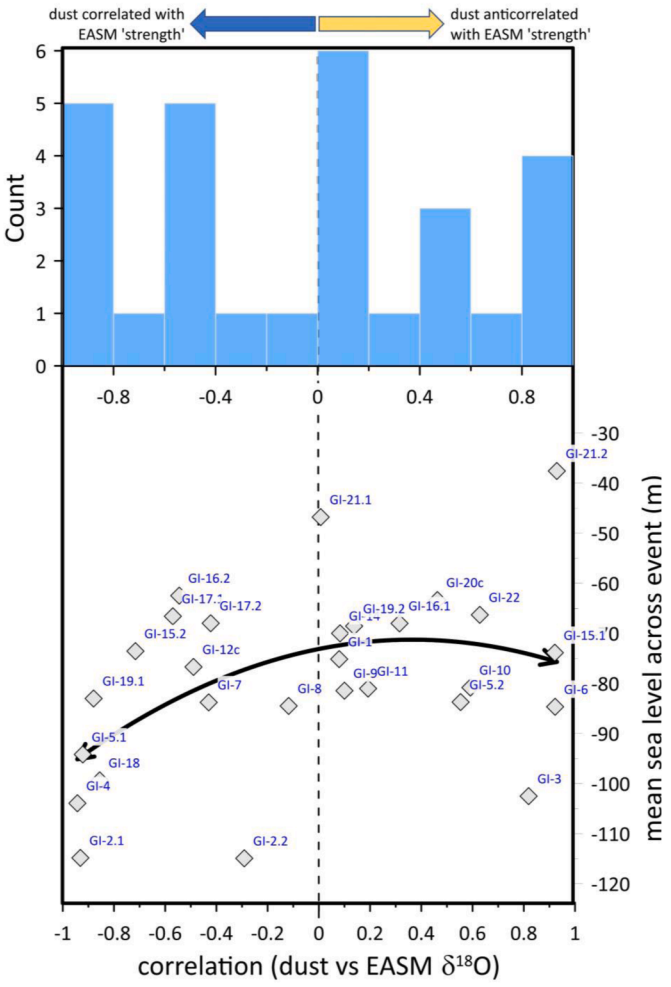

Fig. 7. *Top panel*: A histogram illustrating the number of D-O events with various correlations between EASM δ^{18}O (Cheng et al., 2016) and ^{232}Th East Asia dust flux reconstruction (unsmoothed data). *Bottom panel*: The correlation between EASM δ^{18}O and ^{232}Th East Asia dust flux reconstruction for different events plotted against the mean sea level across the event. Because the more negative stalagmite δ^{18}O values are inversely related to monsoonal strength, negative correlations with the ^{232}Th East Asia dust flux reconstruction represent positive correlations between dust and EASM strength. A second-order polynomial trendline is also shown ($R^2 = 0.21$, $p = 0.01$, $n = 28$) (black line).

westerly wind strength during D-O events, more in-line with expectations of regional increases in moisture reducing dust flux. The somewhat surprising result that at high ice volume conditions SE Asian stalagmite δ^{18}O and dust flux are anticorrelated (Fig. 7), implying that rainfall and dust are correlated, may instead have alternative explanations, as outlined below.

3.4. D-O events within the dust flux reconstruction

SE Asian stalagmite δ^{18}O records preserve evidence for climate shifts associated with North Atlantic D-O events (Figs. 5 and 6). whereas some D-O events are clearly evident within the median ^{232}Th record (e.g., D-O 19.2 and D-O 20), others are not (e.g., D-O 21.1e, Fig. 6) and overall the manifestation of D-O events in the dust record is variable. A D-O event's presence or absence within SE Asian stalagmite δ^{18}O records provides information regarding environmental and climatological changes in SE Asia across these events. Because the δ^{18}O and ^{232}Th datasets are largely obtained from the same stalagmites, we can exclude issues related to location sensitivity to recording these events. It is interesting to note that despite D-O 21 being the longest of the three D-O events discussed here, its expression is absent in the dust record, suggesting that either the event did not result in biome changes in SE Asia (and was atypical), or that the teleconnection between the North Atlantic and SE Asia were different than during the shorter D-O events 19.2 and 20.

The EASM sources 37% of its moisture from the Bay of Bengal (Baker et al., 2016), and we suggest that some D-O events present in the δ^{18}O records do not appear in the dust reconstruction because they predominantly affected Bay of Bengal SST and EASM rainfall δ^{18}O rather than westerly wind position. Alternatively, this could also reflect a stronger EASM but with no dust flux shift, or the fact that D-O event duration was insufficient to change biomes towards those producing dust. However, some D-O events that are not expressed in the SE Asian ^{232}Th median dust flux record are strong and long-lived in Greenland ice cores, which is inconsistent with a more subdued SE Asia dust flux response. Ultimately, the expression of D-O events differs in the EASM domain between events, consistent with recent research (Shi et al., 2022) suggesting that the response partially depends on ice volume and NH summer insolation (Figs. 6 and 7). Regardless, the decoupling of the median stalagmite ^{232}Th record from EASM records during several D-O events suggests that atmospheric reorganisation centred within the North Atlantic did not affect dust flux to SE Asia on these timescales.

3.5. Limitations of the approach

This study suggests that stalagmite ^{232}Th data compilations can be robust proxies for dust flux. However, several limitations to the technique exist. Although median stalagmite ^{232}Th concentrations for intervals with numerous data points appear to faithfully reflect regional dust flux, considerable scatter exists. For intervals with reduced data availability, the results are considerably less reliable due to this lack of

precision. Solutions to this issue include requiring a minimum number of datapoints or ensuring that the selected stalagmites respond to dust flux but not the hydrological transport of detrital material. This would decrease the scatter and increase the precision of the distribution around the median value. Thorium measurements are straightforward via ICP-MS or laser ablation ICP-MS, and if monitoring studies could identify single stalagmites that respond exclusively to aeolian dust flux rather than hydrological detrital inputs (e.g., a slow, diffuse flow-fed stalagmite (Baldini et al., 2021)), continuous dust flux records from a single carefully selected sample might be possible. Lower resolution Sr isotope records across the interval could confirm the robustness of the inferred relationship between ^{232}Th concentrations and dust flux (Cruz et al., 2021). A continuous ^{232}Th dataset from a few carefully selected samples would also circumvent the issue that horizons with elevated ^{232}Th concentrations are under-represented in U-Th dating results.

4. Conclusion

A correlation between recent, compiled stalagmite ^{232}Th concentrations and satellite derived mean DCMD measured above globally distributed cave sites suggests that stalagmite ^{232}Th concentrations are a robust proxy for atmospherically suspended dust. The technique is able to reproduce existing dust flux records when a sufficiently high number of data points exists, albeit with a low precision. This observation permits the application of the large number of published stalagmite ^{232}Th concentration datasets towards the reconstruction of regional paleo-dust fluxes back to 500 ka BP. Because of the long and well-dated records from the region, here we focus on reconstructing dust flux from SE Asia over the last 100 ka.

The ^{232}Th dust flux reconstruction is clearly linked to ice volume, and also tracks EASM δ^{18}O reconstructions from Chinese stalagmites, with dustier intervals linked to less negative stalagmite δ^{18}O (partially reflecting a weaker monsoon). This suggests that SE Asia dust flux is predominantly controlled by westerly wind strength, which in turn tracks larger-scale atmospheric reorganisations linked to ice volume.

Generally, D-O events are apparent in both EASM δ^{18}O record and the median ^{232}Th dust flux reconstruction. However, some D-O events are not expressed in the thorium dust flux reconstruction, such as D-O 21.1e, and the correlation between EASM rainfall and dust flux is variable, possibly reflecting changes in moisture source temperature changes, a decoupling of EASM and dust flux strength, or insufficient event duration for biome change in Central Asia that would result in increased dust production.

This study has tested stalagmite thorium concentrations as a proxy for atmospheric dust flux and found that this technique is viable. U-Th dating of stalagmite carbonate permits a more robust chronology than available for most dust flux archives, and the wide availability of thorium data permits the construction of highly resolved records which complement existing dust flux proxy records. Further refinement of the technique raises the possibility of quantitative and accurately dated dust flux records over at least the past 600 ka.

Declaration of Competing Interest

The authors declare that they have no known competing financial interests or personal relationships that could have appeared to influence the work reported in this paper.

Acknowledgments

We thank two anonymous reviewers for providing comments that greatly improved the manuscript. We also thank Andrew Kerr for their editorial handling of the manuscript. We also thank the SISAL project, and international PAGES working group, for compiling and providing access to the SISAL database v1.

Supplementary materials

Supplementary material associated with this article can be found, in the online version, at doi:10.1016/j.ringeo.2022.100017.

References

Allen, B., 2017. *Atmospheric Aerosols: What Are They, And Why Are They So Important?*. [online] NASA. Available at:https://www.nasa.gov/centers/langley/news/factsheets/Aerosols.html (Accessed 10 August 2022).

Aciego, S., Bourdon, B., Schwander, J., Baur, H., & Forieri, A. (2011). Toward a radiometric ice clock: uranium ages of the Dome C ice core. *Quaternary Science Reviews, 30*, 2389–2397.

Albani, S., Balkanski, Y., Mahowald, N., Winckler, G., Maggi, V., & Delmonte, B. (2018). Aerosol-climate interactions during the last glacial maximum. *Current Climate Change Reports, 4*, 99–114.

Atsawawaranunt, K., Comas-Bru, L., Amirnezhad Mozhdehi, S., Deininger, M., Harrison, S. P., Baker, A., Boyd, M., Kaushal, N., Ahmad, S. M., Ait Brahim, Y., Arienzo, M., Bajo, P., Braun, K., Burstyn, Y., Chawchai, S., Duan, W., Hatvani, I. G., Hu, J., Kern, Z., Labuhn, I., Lachniet, M., Lechleiter, F. A., Lorrey, A., Pérez-Mejías, C., Pickering, R., Scroxton, N., & Sisal Working Group Members. (2018). The SISAL database: A global resource to document oxygen and carbon isotope records from speleothems. *Earth System Science Data Discussion, 2018*, 1–64.

Baldini, J. U. L., Lechleitner, F. A., Breitenbach, S. F. M., van Hunen, J., Baldini, L. M., Wynn, P. M., & Fohlmeister, J. (2021). Detecting and quantifying palaeoseasonality in stalagmites using geochemical and modelling approaches. *Quaternary Science Reviews, 254*, Article 106784. https://doi.org/10.1016/j.quascirev.2020.106784

Baldini, J. U. L., McDermott, F., Baker, A., Baldini, L. M., Mattey, D. P., & Railsback, L. B. (2005). Biomass effects on stalagmite growth and isotope ratios: A 20th century analogue from Wiltshire, England. *Earth and Planetary Science Letters, 240*, 486–494.

Baldini, J. U. L., Baldini, L. M., McDermott, F., & Clipson, N. (2006). Carbon dioxide sources, sinks, and spatial variability in shallow temperate zone caves: evidence from Ballynamintra Cave, Ireland. *Journal of Cave and Karst Studies, 68*, 4–11.

Baldini, JU. L., McDermott, F., Baldini, LM., Ottley, CJ., Linge, KL., Clipson, N., & Jarvis, KE. (2012). Identifying short-term and seasonal trends in cave drip water trace element concentrations based on a daily-scale automatically collected drip water dataset. *Chemical Geology, 330*, 1–16.

Chen, S. Y., Jiang, N. X., Huang, J. P., Xu, X. G., Zhang, H. W., Zang, Z., Huang, K. N., Xu, X. C., Wei, Y., Guan, X. D., Zhang, X. R., Luo, Y., Hu, Z. Y., & Feng, T. C. (2018). Quantifying contributions of natural and anthropogenic dust emission from different climatic regions. *Atmospheric Environment, 191*, 94–104.

Cheng, H., Lawrence Edwards, R., Sinha, A., Spötl, C., Yi, L., Chen, S., Kelly, M., Kathayat, G., Wang, X., Li, X., Kong, X., Wang, Y., Ning, Y., & Zhang, H. (2016). The Asian monsoon over the past 640,000 years and ice age terminations. *Nature, 534*, 640–646.

Choobari, O. A., Zawar-Reza, P., & Sturman, A. (2014). The global distribution of mineral dust and its impacts on the climate system: A review. *Atmospheric Research, 138*, 152–165.

Cruz, J. A., McDermott, F., Turrero, M. J., Edwards, R. L., & Martin-Chivelet, J. (2021). Strong links between Saharan dust fluxes, monsoon strength, and North Atlantic climate during the last 5000 years. *Science Advances, 7*, 26.

Dredge, J., Fairchild, I. J., Harrison, R. M., Fernandez-Cortes, A., Sanchez-Moral, S., Jurado, V., Gunn, J., Smith, A., Spotl, C., Mattey, D., Wynn, P. M., & Grassineau, N. (2013). Cave aerosols: distribution and contribution to speleothem geochemistry. *Quaternary Science Reviews, 63*, 23–41.

GMAO, Global Modeling and Assimilation Office. 2015. "MERRA-2 tavgM_2d_aer_Nx: 2d, monthly mean,time-averaged, single-level, assimilation, aerosol diagnostics V5.12.4." In, edited by Goddard Earth Sciences Data and Information Services Center (GES DISC). Greenbelt, MD, USA.

Guo, Z. T., Berger, A., Yin, Q. Z., & Qin, L. (2009). Strong asymmetry of hemispheric climates during MIS-13 inferred from correlating China loess and Antarctica ice records. *Climate of the Past, 5*, 21–31.

Hellstrom, J. (2003). Rapid and accurate U/Th dating using parallel ion-counting multi-collector ICP-MS'. *Journal of Analytical Atomic Spectrometry, 18*, 1346–1351.

Huybers, P. (2006). Early Pleistocene glacial cycles and the integrated summer insolation forcing. *Science, 313*, 508–511.

James, E. W., Banner, J. L., & Hardt, B. (2015). A global model for cave ventilation and seasonal bias in speleothem paleoclimate records. *Geochemistry, Geophysics, Geosystems, 16*, 1044–1051. https://doi.org/10.1002/2014GC005658

Jamieson, R. A., Baldini, J. U. L., Frappier, A. B., & Muller, W. (2015). Volcanic ash fall events identified using principle component analysis of a high-resolution speleothem trace element dataset. *Earth and Planetary Science Letters, 426*, 36–45.

Lisiecki, L. E., & Raymo, M. E. (2005). A Pliocene-Pleistocene stack of 57 globally distributed benthic delta O-18 records. *Paleoceanography, 20*, Article PA1003. https://doi.org/10.1029/2004PA001071

Liu, T. S., An, Z. S., Yuan, B. Y., & Han, J. M. (1985). The loess-paleosol sequence in china and climatic history. *Episodes, 8*, 21–28.

Martinez-Garcia, A., Sigman, D. M., Ren, H. J., Anderson, R. F., Straub, M., Hodell, D. A., Jaccard, S. L., Eglinton, T. I., & Haug, G. H. (2014). Iron fertilization of the subantarctic ocean during the last ice age. *Science, 343*, 1347–1350.

Mikami, M., Shi, G. Y., Uno, I., Yabuki, S., Iwasaka, Y., Yasui, M., Aoki, T., Tanaka, T. Y., Kurosaki, Y., Masuda, K., & Uchiyama, A. (2006). Aeolian dust experiment on climate impact: An overview of Japan–China joint project ADEC. *Global and Planetary Change, 52*(1-4), 142–172.

Miller, R. L., Knippertz, P., Pérez García-Pando, C., Perlwitz, J. P., Tegen, I., Stuut, J. B., & Knippertz, P. (2014). Impact of dust radiative forcing upon climate. Ed.. *Mineral dust* Dordrecht: Springer

NGICP Members. (2004). High-resolution record of Northern Hemisphere climate extending into the last interglacial period. *Nature, 431*, 147–151.

Shi, X., Yang, Y., Cheng, H., Zhao, J., Li, T. Y., Lei, L., Liang, S., Feng, X., & Lawrence Edwards, R. (2022). Influences on Asian summer monsoon during Dansgaard-Oeschger events 19 to 25 (70–115 kyr B.P.). *Palaeogeography, Palaeoclimatology, Palaeoecology, 587*, Article 110798.

Siddall, M., Rohling, E. J., Almogi-Labin, A., Hemleben, C., Meischner, D., Schmelzer, I., & Smeed, D. A. (2003). Sea-level fluctuations during the last glacial cycle. *Nature, 423*, 853–858.

Ujvari, G., Kovacs, J., Varga, G., Raucsik, B., & Markovic, S. B. (2010). Dust flux estimates for the last glacial period in East Central Europe based on terrestrial records of loess deposits a review. *Quaternary Science Reviews, 29*, 3157–3166.

Vaks, A., Bar-Matthews, M., Matthews, A., Ayalon, A., & Frumkin, A. (2010). Middle-late quaternary paleoclimate of northern margins of the Saharan-Arabian Desert: Reconstruction from speleothems of Negev Desert, Israel. *Quaternary Science Reviews, 29*, 2647–2662.

Wong, C. I., & Breecker, D. O. (2015). Advancements in the use of speleothems as climate archives. *Quaternary Science Reviews, 127*, 1–18.

Yancheva, G., Nowaczyk, N. R., Mingram, J., Dulski, P., Schettler, G., Negendank, J. F. W., Liu, J. Q., Sigman, D. M., Peterson, L. C., & Haug, G. H. (2007). Influence of the intertropical convergence zone on the East Asian monsoon. *Nature, 445*, 74–77.